

This work has been submitted to American Meteorological Society's Journal of Climate and is currently undergoing review. Copyright in this work may be transferred without further notice. Subsequent versions may have different content. If the manuscript gets accepted, the peer reviewed version will be available via the DOI link. We welcome feedback, please do not hesitate to contact us.

ABSTRACT

11 We propose a metric for measuring internal and forced variability in ensemble atmosphere, ocean,
12 or climate models using information theory: Shannon entropy and mutual information. This metric
13 differs from the standard ensemble-variance approaches. Information entropy quantifies variability
14 by the size of the visited probability distribution, as opposed to variance that measures only its
15 second moment. Shannon entropy and mutual information manage correlated fields, apply to any
16 data, and are insensitive to outliers as well as a change of units or scale. Finally, we use an example
17 featuring a highly skewed probability distribution (Arctic sea surface temperature) to show that
18 the new metric is robust even with a sharp nonlinear cutoff (the freezing point). We apply these
19 two metrics to quantify internal vs forced variability in (1) idealized Gaussian data, (2) an initial
20 condition ensemble of a realistic coastal ocean model, (3) the Community Earth System Model
21 large ensemble. Each case illustrates the advantages of the proposed metric over variance-based
22 metrics. Furthermore, in the coastal ocean model, the new metric is adapted to further quantify
23 the impact of different boundary forcing choices to aid in prioritizing model improvements—i.e.,
24 comparing different choices of extrinsic forcing. The metric can be applied to any ensemble of
25 models where intrinsic and extrinsic factors compete to control variability and can be applied
26 regardless of if the ensemble spread is Gaussian.

27 **1. Introduction**

28 In an ocean or climate model, it is pertinent to understand the cause of variability as it leads to
29 implications for predictability, prioritization of data collections for assimilation, and provides an
30 understanding of the dynamics at play in different regions. In a coastal model, variability can arise
31 from extrinsic factors such as wind forcing, solar and thermal forcing, tides, rivers, evaporation and
32 precipitation, or it can be due to internal chaos inherent to the governing fluid equations (Sane et al.
33 2020). In a climate model, modes of variability such as El Niño, the North Atlantic Oscillation,
34 or the Southern Annular Mode, can conceal or delay the emergence of attributable anthropogenic
35 climate change signals (Milinski et al. 2019). In high-resolution ocean models, internal chaos or
36 intrinsic variability can also be due to eddies (Leroux et al. 2018; Llovel et al. 2018). Accurately
37 quantifying the relative contribution of external and internal factors can help in elucidating the
38 causes responsible for the observed variability in models, help to identify key observable metrics,
39 and help quantify concepts such as the time of emergence of climate signals (Hawkins and Sutton
40 2012).

41 Numerous methods exist in the literature to quantify intrinsic and extrinsic variability using
42 models or observations (e.g., Frankcombe et al. 2015; Schurer et al. 2013; Liang et al. 2020).
43 Model ensembles—i.e., a set of simulations sharing the same forcing—naturally vary because each
44 ensemble member follows the same governing equation (with same external forcings) with identical
45 or similar parameterizations but differ due to intrinsic chaos. Two types of model ensembles are
46 common: initial condition ensembles (where the same model is used repeatedly with perturbed
47 initial conditions and intrinsic variability occurs from model’s chaotic sensitivity to the initial
48 conditions), and multi-model ensembles (where a variety of models differing in numerics and
49 parameterizations are used to simulate change under the same forcing—in this case “intrinsic”

50 variability also includes aspects of model formulations). Most of the discussion here will focus on
51 initial condition ensembles, but the metrics proposed can be adapted to both cases.

52 To help visualize variability, a generic output from an ocean or atmospheric model is shown in
53 Figure 1. Each color represents a different ensemble member and the black solid line is the mean of
54 those members. The black solid line is the signal mostly due to extrinsic factors (aside from finite
55 ensemble size limits) and the model spread (schematized by the double-headed magenta arrow in
56 Figure 1) can be considered due to intrinsic variability or internal chaos.

57 One method of quantifying intrinsic and extrinsic variability is to look at variances (second
58 central statistical moment) of model spread and model mean (Leroux et al. 2018; Llovel et al.
59 2018; Waldman et al. 2018; Yettella et al. 2018). Variance is sufficient to constrain all metrics of
60 variability about the mean when distributions are Gaussian and uncorrelated, but a single statistical
61 moment usually measures only part of a more complex variability. Many climatological variables
62 show non-Gaussian distributions (e.g., Franzke et al. 2020). In fact, generalized variance might
63 be misleading (Kowal 1971). Quantification of variability should be robust to or have known
64 dependence on changes in the units of the quantity or the scale (e.g., changing temperature from
65 Celsius to Fahrenheit or Kelvin). Comparative metrics, such as intrinsic vs. extrinsic variability
66 should not depend on these arbitrary choices of units at all.

67 Variability, in essence, is a function of the number of occurrences or frequency of occurrence
68 (or probability p_i as a fraction over all visited system states) after appropriately binning the data
69 (and thereby making the estimated and visited number of states finite rather than continuous).
70 Information entropy metrics measure variability by taking into account the probability distribution
71 of the binned data, drawing on the statistical mechanics concept of entropy in quantifying the
72 number of microstates that a variable can occupy. The fundamental measure in information theory
73 is the Shannon (1948) or information entropy which characterizes the amount of variability in a

74 variable (Carcassi et al. 2019). The mutual information, another metric introduced by Shannon
75 (1948), measures how much information one variable contains about another variable.

76 Information theory is applied in signal processing, computer science, statistical mechanics,
77 quantum mechanics, etc. It is used to quantify amount of information, disorder, freedom, or lack
78 of freedom (Brissaud 2005). The application of these abstract notions to geophysical flows can
79 have immense practical benefit when information entropy is interpreted as a measure of variability,
80 as entropy does not rely on any particular parametric probability distribution. Metrics from
81 information theory are not new to climate sciences. They have been introduced in predictability
82 studies, evaluating the skill of statistical models, as well as uncertainty studies (e.g., Leung and
83 North 1990; Schneider and Griffies 1999; Kleeman 2002; DelSole and Tippett 2007; Majda and
84 Gershgorin 2010; Stevenson et al. 2013).

85 In this article we bring well-established concepts of information theory to the particular applica-
86 tion of measuring intrinsic and extrinsic variability for ensemble model runs within atmospheric
87 and oceanographic modeling. Our metric uses Shannon entropy and mutual information together,
88 which we explain in section 2. We will apply our metric on three sets of data in section 3: 1.
89 Idealized Gaussian arrays with specified correlation 2. Ensemble output of a regional coastal
90 model (OSOM) (Sane et al. 2020) where output is mostly non Gaussian. 3. Community Earth
91 System Model Large ensemble (Deser et al. 2020). In section 4, we use individual components of
92 our metric to compare simulations from differing forcings applied to OSOM.

93 **2. Information theory**

94 We will introduce information theory concisely assuming the reader has no background
95 knowledge—this section contains standard definitions. Consider a probability distribution p_i ob-
96 tained after binning data into N bins. The user chooses the appropriate number of bins or bin

97 widths for the range of data. Shannon (1948) identified the average information content in N
98 possible outcomes, equally or not equally likely, as given by:

$$H = \sum_{i=1}^N p_i \log_2(1/p_i), \quad (1)$$

99 where H is the Shannon entropy with unit of bits when log is base 2 and p_i is the probability of
100 the i^{th} outcome. $\log_2(1/p_i)$ measures the information of the i^{th} outcome as proposed by Hartley
101 (1928) and is also a measure of uncertainty (Cover 1999). The quantum $\log_2(1/p_i)$ measures
102 the information gained by knowing that the i^{th} outcome has happened. Another interpretation for
103 $\log_2(1/p_i)$ is that it measures reduction in uncertainty by knowing the i^{th} event has occurred, or
104 that the variable falls in the i^{th} bin. The term information does not mean knowledge but it means
105 the amount of uncertainty shown by a variable or the freedom that a variable has in falling into
106 the i^{th} out of the N bins. Shannon (1948) found Equation 1 to provide the average information (or
107 uncertainty) for all events in a record. For the entire set of elements, a highly probable event has
108 less uncertainty associated with it and low probability event has high uncertainty associated with it.
109 The prefactor p_i is thus used to weight the information over all possibilities. One way to interpret
110 the need for the prefactor p_i is that in repeated experiments the events with higher probability
111 will occur more often, hence they should contribute more to a quantification of variability than
112 infrequent events.

113 Stone (2015) gives an intuitive way of understanding Shannon entropy using a binary tree.
114 A binary tree is a tree chart which starts with 1 node and splits to two nodes at each node.
115 At each node you can take a left or right turn to proceed and if there are say 3 levels in the
116 tree, then 8 (i.e. 2^3) outcomes or possible destinations exist. If a binary tree has N equally
117 probable outcomes then the set of instructions required to reach the correct destination is given by
118 $h = (N)(1/N) \log_2(N) = \log_2(N)$. The *uncertainty* about reaching the correct destination will be

119 removed by providing $\log_2(N)$ bits of information. In other words, if entropy is h then 2^h states
120 are possible.

121 A second metric from Shannon (1948) which is also extensively used is now known as *mutual*
122 *information*. The mutual information between two signals x and y denoted by $I(X;Y)$ is (Cover
123 1999)

$$I = \sum_{j=1}^N \sum_{i=1}^N p_{ij} \log_2 \left(\frac{p_{ij}}{p_i p_j} \right), \quad (2)$$

124 where p_{ij} is joint probability of i^{th} outcome of x and j^{th} outcome of y . p_i and p_j is the marginal
125 probability of i^{th} and j^{th} outcome of x and y respectively. The addend within the summations can
126 be expanded to $p_{ij} (\log_2(p_{ij}) - \log_2(p_i) - \log_2(p_j))$. I can be interpreted as the extra information
127 in entropy of marginal distributions of x and y over joint distribution. Mutual information is
128 symmetric between x and y and is the measure of how much information they share. For example,
129 if the distributions are statistically independent, then $p_{ij} = p_i p_j$ and thus $I = 0$. If the two records
130 x and y are identical, then $p_{ij} = p_i = p_j$ and $I = H$. I is the average reduction in uncertainty in
131 x by knowing y or vice versa. It denotes how much information is transmitted between the two
132 variables.

133 In the context of ocean modeling (or in general climate modeling) entropy is used to measure
134 variability in a model output or available data. This is in tandem with interpretation of Shannon
135 entropy in physical sciences as given in Carcassi et al. (2019). When calculating the Shannon
136 entropy we are concerned about the possible states (for e.g. the various bins in a histogram) the
137 variable can (and does) go into while the variable value and its dimensions are of lesser importance.
138 Entropy metrics measure variability in *bits* (when logarithm is of base 2) and hence changing the
139 scale, for e.g. switching from Celsius to Fahrenheit for temperature, does not change the value
140 of variability (under equivalent binning). Mutual information and entropy are both dimensionally

141 agnostic. They are also not sensitive to outliers (due to the weighting prefactor) and can capture non
 142 linear interactions (Correa and Lindstrom 2013) and discontinuous or intermittent visited states.
 143 We will present the effect of correlation and outliers in section 3 a.

144 3. Proposed metric

145 Let $f(t)^i$ denote ensemble output as a function of time t and i is the index of ensemble members.
 146 For ocean model simulations, the output signal $f(t)^i$ consists of trend due to external forcing
 147 given by $g(t) = \langle f(t)^i \rangle$ where angled brackets represent mean over the ensemble members and
 148 the remaining part is the intrinsic variability due to chaos given by $\eta(t)^i$. Typically, g would be
 149 estimated as the mean of the ensemble, but in some cases might be a median or a known response
 150 to forcing—another advantage of the information theory approach is that it is not required that g
 151 be the mean or that $\eta(t)^i$ have no mean value. Thus they are related as $f(t)^i = g(t) + \eta(t)^i$, where
 152 $g(t)$ represents the forced component of the total variability and the model spread $\eta(t)^i$ can be
 153 attributed to the internal chaos (or model distinctions in multi-model ensembles) (e.g., Waldman
 154 et al. 2018; Llovel et al. 2018).

155 Usually we are limited in the number of ensemble members due to computational costs so we
 156 perform a *jugaad* with f and g in order to use all the members at once to sample widely and obtain
 157 an accurate probability distribution. Let f be a single array obtained by combining (concatenating)
 158 all members $f(t)^i, \forall i \in N$, where N is the total number of ensemble members. Let g be the array
 159 obtained after copying the model mean $g(t)$ N times. Hence if there are M data points in each
 160 member, f and g are of length $N \times M$ each. This makes them of equal length and the metric can
 161 be applied to the whole ensemble output. Using f and g , we propose the following metric γ

$$\gamma = 1 - \frac{I(f;g)}{H(f)}, \quad (3)$$

162 $H(f)$ is the Shannon entropy of f and $I(f;g)$ is mutual information between f and g . Note that
 163 g is due to extrinsic factors and f is obtained after internal chaos adds to g . $I(f;g)$ calculates
 164 the contribution of extrinsic signal g to the whole ensemble. $H(f)$ is the total variability in the
 165 ensemble output which is culmination of extrinsic and intrinsic factors. The metric γ gives the
 166 *ratio of intrinsic variability to total variability*.

167 $H(f)$ and $I(f;g)$ are related through conditional entropy by $H(f) = I(f;g) + H(f|g)$ (Cover
 168 1999). $H(f|g)$ is the conditional entropy¹, i.e., average uncertainty about the value of f after g
 169 is known. It is the uncertainty in f that is not attributed to g but is attributed to noise η . Hence
 170 $H(f) - I(f;g)$ determines variability due to intrinsic chaos.

171 Returning to the binary tree analogy, $I(f;g)$ would be the set of instructions sent by a source
 172 to reach one among $2^{H(f)}$ possible destinations in the presence of noise having $H(f|g)$ entropy.
 173 To capture the entropy in the noisy binary tree, to each of the $2^{I(f;g)}$ microstate possibilities noise
 174 $(2^{H(f|g)})$ gets multiplied and the relation becomes $2^{H(f)} = 2^{I(f;g)}2^{H(f|g)}$.

175 $I(f;g)$ takes into account any correlation or information shared between f and g . This is vital
 176 because even though the model spread η is being treated similarly to noise added to the mean
 177 signal, it might be that model spread depends on the mean signal. A simple example is if the model
 178 spread is relative (e.g., 10% of the mean signal), rather than absolute (e.g., 2 units), then there
 179 is information about the model spread contained in the mean signal. This situation is sometimes
 180 called multiplicative noise in contrast to additive noise. The nonlinear and chaotic nature of fluid
 181 mechanics often leads the mean flow to amplify the chaotic signal (e.g., eddies) and thereby result
 182 in altered variability statistics. When $f \rightarrow g$, then $I(f;g) \rightarrow H(f) = H(g)$ from (2). This makes
 183 $\gamma = 0$ when there is no intrinsic chaos. When intrinsic chaos fully dominates the ensemble output,

¹Conditional entropy $H(X|Y)$ is defined by $H(X|Y) = \sum p(x|y)\log_2 p(x|y)$ (Cover 1999). It is not necessary to calculate conditional entropy to arrive at γ , but understanding is aided by the expected relation between entropy and mutual information.

184 i.e. f and g are fully decorrelated, then $I(f;g) = 0$ yielding $\gamma = 1$. We see that γ satisfies the
185 extremes of zero noise as well as total chaos.

186 Another analogy for a climate system component is a noisy channel as given in Leung and
187 North (1990), where the governing equations of ocean (atmosphere) modeling are represented
188 by a channel. The extrinsic forcings are inputs to the channel, the intrinsic chaos is the noise
189 created because of channel's inherent mechanisms while the outputs are the ensemble members.
190 A noiseless channel will give γ as zero and completely noisy channel where output is independent
191 of input will yield γ as 1.

192 A seemingly enticing and simpler alternative is $\gamma = 1 - \frac{H(g)}{H(f)}$, i.e. just the difference between
193 ensemble entropy and mean entropy as a ratio with the ensemble entropy. However, this formulation
194 is incorrect because $H(g)$ does not quantify the contribution of extrinsic factors to the variability
195 in the ensemble, it only quantifies the variability of the mean. Relatedly, $H(f) - H(g)$ does not
196 correctly manage mutual information between the ensemble members and their mean in estimating
197 the intrinsic variability.

198 *a. Idealized Gaussian Arrays*

199 We test our metric, γ , from (3) on synthetic data consisting of idealized arrays of Gaussian
200 data: $\mathcal{N}(0, 1)$. For a normal Gaussian distribution Shannon entropy depends² only on the standard
201 deviation σ i.e. $H = \log_2(2\pi e\sigma^2)$. The variability in a Gaussian distribution can be increased
202 or decreased by changing its standard deviation. To illustrate, we compare our metric γ with the

² $H = \log_2 2\pi e\sigma^2$ is the Shannon entropy of a Gaussian distribution when probability density is continuous with σ as standard deviation. The Shannon entropy of a discrete probability distribution differs, which is inconsequential here but the reader is encouraged to read Jaynes (1962). Consistently here discretely sampled and binned probability distributions are obtained directly from data without any further parameterization.

203 traditional metric of intrinsic versus extrinsic variability γ_{std} :

$$\gamma_{std} = \frac{\sigma_i}{(\sigma_i^2 + \sigma_g^2)^{1/2}}, \quad (4)$$

204 where subscript *std* stands for standard deviation, σ_i is the temporal mean of standard deviation
205 of model spread, and σ_g is the temporal standard deviation of the model mean (not a function of
206 time). Our goal is to compare γ and γ_{std} . We set out our numerical experiment as follows: we
207 create 10 arrays, each having 10,000 elements drawn from a Gaussian distribution. Any two arrays
208 from those 10 have a prescribed linear Pearson correlation coefficient from 0 to 1.

209 Thus, the 10 arrays covary linearly with a specified correlation coefficient. These 10 arrays
210 represent each of 10 ensemble members from climate simulations. The mean of 10 members
211 gives us the synthetic forced variability signal as would be determined from the model output;
212 averaging over the 10 ensemble members reduces the contribution from uncorrelated variability
213 and reaffirms the covarying component into the forced variability. As the individual members
214 have same correlation coefficient between them, every member also has a constant correlation
215 (different from correlation between any two ensemble members) with the mean member. We apply
216 γ and γ_{std} on this synthetic ensemble by varying the prescribed correlation coefficient from 0 to 1.
217 Figure 2 shows that as expected both metrics increase as the correlation decreases, i.e., as internal
218 variability dominates forced. Both metrics behave similarly when correlation decreases, i.e. noise
219 increases but γ is more sensitive as correlation tends to 1. This distinction is due to the logarithmic
220 nature of Shannon entropy for Gaussian distributions—in essence, information measured in bits
221 is not proportional to distance measured between distributions in terms of summed variance—in
222 the examples following the consequences of this distinction will become clearer. Critically both
223 functions are monotonic with correlation, however so relative comparisons (more intrinsic fraction
224 in this region vs. that region) are preserved.

225 A second related experiment was derived from the first is also shown in Figure 2: adding outliers
226 outside of the Gaussian distribution. 50 out of 10000 elements of each individual member were
227 artificially corrupted (values were set to a constant value of 5) to test the sensitivity of both the
228 metrics. Figure 2 shows that γ is insensitive to outliers while γ_{std} is not. γ is not sensitive because
229 outliers occur less frequently and hence do not affect the probability distribution much, especially
230 with the prefactor in (1) and (2). Hence information theory metrics are robust in comparison to
231 using standard deviation (or variance). If the outliers (extreme events) occur at higher frequencies,
232 information metrics will naturally start sensing them even if they are discontinuous from the typical
233 conditions (e.g., multimodal distributions). Increasing the number of ensemble members does not
234 change the result qualitatively for both the experiments.

235 *b. Regional coastal model output*

236 In this section we show the results of applying γ and γ_{std} on realistic simulation data from the
237 Ocean State Ocean Model, hereafter OSOM (Sane et al. 2020). OSOM uses the Regional Ocean
238 Modeling System (ROMS) (Shchepetkin and McWilliams 2005) to model Narragansett Bay and
239 surrounding coastal oceanic regions and waterways. OSOM’s primary purpose is for understanding
240 and predictive modeling and forecasting of the estuarine state and climate of this Rhode Island
241 body. Sane et al. (2020) gives more details about the model.

242 Using OSOM, an ensemble of simulations have been performed using perturbed initial conditions
243 for the months July - August of 2006. The data during the initial predictability window (20 days)
244 has been ignored and the rest has been used to look at variability within the “climate projection”
245 of the model beyond when forecasts sensitive to initial conditions are possible (see the related
246 application of information theory to assess predictability in Sane et al. 2020). We examine whether
247 the modeled temperature and salinity at each grid point follow normal distributions by evaluating

248 the skewness and kurtosis of the model mean at each grid point. Figure 3 shows skewness and
249 kurtosis for sea surface salinity and temperature as well as bottom salinity and temperature for the
250 Narragansett Bay region. The horizontal axis shows skewness and excess kurtosis, which are the
251 third and fourth statistical moments respectively, normalized by powers of the standard deviation
252 to dimensionless ratio and in the case of excess kurtosis a constant value of 3 is subtracted. For
253 Gaussian distributions, skewness and excess kurtosis both should be close to zero. The vertical axis
254 denotes the number of occurrences at a grid point. Observe that the majority of grid point values
255 are away from zero. These variables are considerably non-Gaussian in OSOM. Thus, (4) is at a
256 disadvantage, because the prevalence of higher statistical moments implies that the variance does
257 not contain a complete description of the variability. The information theory metric (3) is suitable
258 for such data as it takes into account higher moments and does not rely on Gaussian distributions.

259 Figure 4 shows the ratio of intrinsic variability to total variability applied on every grid point
260 for OSOM. γ is displayed on left whereas γ_{std} is shown on right for comparison. The features
261 highlighted by both metrics are qualitatively different. The contribution of intrinsic chaos to total
262 variability is more uniform using the γ metric than using γ_{std} . The intrinsic chaos displayed using
263 γ_{std} might be misleading because the probability distributions are non-Gaussian. Furthermore,
264 where the γ metric highlights internal variability tends to agree in similar dynamical locations—all
265 river mouths show high surface salinity intrinsic variability, while surface temperature intrinsic
266 variability is higher in more open regions of the Bay where eddies form from topography intermit-
267 tently. Also note that the ranges are quite different between γ and γ_{std} , but this is to be expected
268 from the different rate of increase with correlation seen in Figure 2.

269 *c. Community Earth System Model large ensemble*

270 A complementary experiment was performed by using γ to evaluate internal vs. forced variability
271 in the global climate simulation output for climate change scenario RCP8.5 using the (randomly
272 selected among the models compared) GFDL CM3 model (Deser et al. 2020). Variability of sea
273 surface temperature (Figures 5) as well as sea surface salinity (6) were estimated using both γ and
274 γ_{std} (upper left and upper right). The skewness and excess kurtosis of the model mean were also
275 plotted to find the deviation of variables away from Gaussian distributions (lower). Regions shaded
276 in purple have low values of excess kurtosis and skewness and might be considered Gaussian.

277 Note in particular the Arctic sea surface temperatures, which have a highly skewed and excessive
278 kurtosis distribution due to the freezing point of seawater. The standard metric deems this region
279 to be among the most intrinsically variable in the world, while the information theory metric has
280 it as a low intrinsic variability region. It is clear that a Gaussian metric should not be applied to
281 this region, and the inference is opposite using the two metrics. In the equatorial Pacific where
282 Gaussian statistics are more reliable, the two metrics agree that internal variability is high.

283 A less drastic failure occurs from the modest excess kurtosis in extra-tropical temperatures and
284 in a few isolated regions in surface salinity. These regions are also non-Gaussian, but also are
285 not heavily skewed (i.e., they are more long-tailed and intermittent than Gaussian). These regions
286 differ in relative estimation of intrinsic versus total variability. It is also the case that the γ metric
287 is closer to one in most regions than γ_{std} , which is to be expected when the correlation coefficients
288 are low from Figure 2.

289 **4. Quantifying extrinsic factors**

290 In section 3 we proposed our metric and showcased its applications. Here instead of us-
291 ing the new metric γ , we use its components: Shannon entropy and mutual information in-

292 individually to compare variability between different simulations. Quantifying differences be-
293 cause of changes in the extrinsic forcings may be required for coastal applications where sys-
294 tems vary predominantly due to external forcings (note that intrinsic variability is less than
295 half by both metrics in Figure 4). For these forcing significance experiments, OSOM was
296 run after modifying the external forcings (Table 1). OSOM is forced by tides, river runoff,
297 atmospheric winds and air-sea fluxes, etc. (Full details of the model can be found in Sane
298 et al. 2020). For this comparison, we quantify the effects of altering forcing on 4 modeled
299 variables: sea surface temperature and salinity, and bottom temperature and salinity. Four al-
300 tered forcing sets were utilized, beyond set (1) Full set of atmospheric forcings using the North
301 American Mesoscale (NAM) analyses, a data-assimilating, high resolution (12 km) meteorologi-
302 cal simulation ([https://www.ncei.noaa.gov/data/north-american-mesoscale-model/
303 access/historical/analysis](https://www.ncei.noaa.gov/data/north-american-mesoscale-model/access/historical/analysis)) denoted as FF. FF stands for full forcing. (2) Full set of at-
304 mospheric forcings but using the Northeast Coastal Ocean Forecast System (NECOFS) winds
305 (Beardsley and Chen 2014) instead of NAM, denoted as NECOFS. (3) River flows are replaced
306 with their monthly-averaged flow, other forcing as in FF (4) River flows set to zero, other forcing
307 as in FF. (5) Wind forcing set to zero, other forcing as in FF. These forcings have been tabulated in
308 Table 1. The aim is to quantify the effect on total variability by removing or altering one of many
309 processes which might contribute.

310 We show results in Figures 7 and 8. Entropy has been plotted with respect to time. In Figure 7,
311 Shannon entropy is plotted for spatial quantities. For example, for surface salinity, all the surface
312 values have been considered to find Shannon entropy. Figure 8 displays mutual information.
313 Mutual information has been calculated in the following way: for surface temperature comparison
314 between FF and MR, surface grid point values for FF simulation were ordered and put in a single
315 row array. We compared this array with a similar array made of surface grid point values of MR

316 surface temperature. We consistently followed the same method for all the forcings and variables.
317 It is user's choice to choose the type of domain, here we have chosen the same domain of OSOM
318 as shown in figure 4. If Shannon entropy is more or less equal for two forcings, it implies they
319 similarly affect variability. Mutual information should be compared for two pairs of forcings.
320 Greater mutual information implies the two pairs share more *bits* of information, suggesting one
321 of the forcing in that pair can be replaced with the other without significantly affecting variability.

322 5. Discussion

323 Our numerical experiments performed using γ on idealized Gaussian arrays show that γ is
324 monotonic and decreases as the linear Pearson correlation coefficient increases. Thus aside from
325 the qualitative differences the new metric finds when the data are non-Gaussian, the ranges of
326 intrinsic versus total variability are quite different between γ and γ_{std} . This is to be expected from
327 the different rates of increase with correlation seen in Figure 2. Approximately, the traditional
328 metric falls approximately linearly as the correlation coefficient increases, so that a correlation
329 coefficient of 0.5 gives a γ_{std} just above 0.5. The new metric γ agrees with γ_{std} that correlation
330 of 0 implies $\gamma = 1$, and correlation of 1 implies $\gamma = 0$, but correlation of 0.5 is closer to $\gamma = 0.9$.
331 Only very near correlation coefficients of 1 does γ fall below 0.5. If roughly linear dependence on
332 correlation coefficient is desired, γ can be raised to a power— γ^3 resembles γ_{std} and γ^6 resembles the
333 correlation coefficient. These higher powers do not lose the ability to apply to non-Gaussian data
334 nor become non-monotonic, but they will lose their interpretation as a ratio of bits of information
335 entropy, and instead reflect ratios of bits cubed of information entropy, etc. An alternative is to
336 take γ_{std} raised to a different power: $\gamma_{std}^{1/3}$ is roughly similar to γ .

337 As can be seen in Figures 4, 5, and 6, information theory metrics show different patterns as
338 compared to variance. Information theory metrics, especially mutual information, account for

339 *all* non-linear shared information between the ensemble members and the mean including linear
340 correlation, and this is one reason for the differences. We have argued that non-Gaussian statistics
341 are another (which is not wholly independent of non-linear shared relationships). There are likely
342 other aspects of differences between these metrics, but the management of these two expected
343 aspects of geophysical fluids–nonlinear relationships and non-Gaussian distributions–justify the
344 introduction of the new metric.

345 For the regional coastal model OSOM, forcings differ as to how they affect different variables.
346 As might be expected, river runoff is more important for salinity than for temperature. How-
347 ever, replacing rivers with the monthly-mean river flow gives nearly the same result (in terms of
348 variability) as fully time-varying rivers. For the duration considered (July-August), averaging the
349 river runoff gives similar effect for salinity as compared to giving the observed river runoff in the
350 simulations, see Figure 7. Temperature is less sensitive to any of the forcing alterations, because
351 although temperature and salinity are passive tracers they have different sources and sinks. Switch-
352 ing the wind product from NAM to NECOFS does not have any significant effect on the sources
353 or sinks of temperature or salinity, but switching the wind off definitely affects the parameters by
354 eliminating wind-driven mixing altogether. Figure 8 shows that zero wind (ZW) simulations are
355 markedly different than the rest in terms of *mutual information* (i.e., they do not covary), although
356 very similar in terms of amount of variability (Shannon entropy, Figure 7), because even without
357 winds tides, fluxes, and rivers still vary. The zero river case tends to eliminate both variability and
358 mutual information (ZR). Please note that our simulations are for July-August, and results might
359 be different for different season.

360 If we were to prioritize improvements based on Shannon entropy and mutual information, note
361 that the two highest mutual information cases are where NAM is substituted with NECOFS and
362 where mean rivers are substituted for varying rivers. The first observation is important from a

363 forecast perspective, because it means that we can not easily tell the difference between different
364 wind products, although something rather than zero winds should be used if the estuary is forecast
365 out to the full 20 day predictability range (weather forecasts only good out about 7 days in this
366 region). Similarly, knowing that substituting the mean of the rivers for the fully varying rivers
367 has little impact implies that rivers can be fixed in time for forecasts beyond where they might be
368 predicted based on expected weather and precipitation. Finally, despite the fact that Narragansett
369 Bay is a dominantly tidally-mixed estuary, among the sources of overall variability (i.e., sources
370 of information entropy) considered, preserving an inflow of fresh water is key, even though that
371 inflow can be steady. Winds do not appreciably increase information entropy of the Bay, but they
372 are an important source of forced co-variation, and so are important for predictions but do not raise
373 the overall level of variability.

374 **6. Conclusion**

375 We have proposed an information theory metric to determine contribution of intrinsic chaos and
376 external variability to total variability in ensemble model simulations. Our metric uses Shannon
377 entropy and mutual information and has several advantages over using only standard deviation (or
378 variance). We have applied our metric on idealized Gaussian arrays as well as realistic coastal
379 ocean and global climate model. We conclude that:

- 380 1. The new information theory metric is more reliable when outliers are present, because out-
381 liers get assigned less probability and because Gaussian distributions have a difficult time
382 approximating long-tailed (i.e., outlier prone) distributions.
- 383 2. The new information theory metric is more reliable when variability is non-Gaussian because
384 it is based on non-parametric measures of the probability distributions.

- 385 3. The new information theory metric varies monotonically with ensemble member to ensemble
386 mean correlation, but is quantified in fraction of bits required to capture internal variability
387 versus bits required to capture of total variability.
- 388 4. The use of the information theory metric in a coastal ocean model ensemble and a climate
389 model ensemble qualitatively changes the focus to regions that were previously erroneously
390 labeled as having high or low internal variability.
- 391 5. In this case, the coastal ensemble had a much smaller intrinsic (chaotic) proportion of its
392 total variability in comparison to the climate ensemble had more intrinsic (weather, climate
393 oscillations, etc.) as a proportion of its total. Importantly, the resolution of the models helps
394 determine the proportion of intrinsic variability, so such comparisons are model-specific:
395 a higher resolution coastal model might well have a larger intrinsic fraction than a coarser
396 climate model.

397 *Acknowledgments.* The Rhode Island Coastal Ecology Assessment Innovation & Modeling grant
398 (NSF 1655221) supported this work. BFK was also supported by ONR N00014-17-1-2963 and
399 NSF 1350795. This material is based upon work conducted at a Rhode Island NSF EPSCoR
400 research facility Center for Computation and Visualization (Brown University), supported in part
401 by the National Science Foundation EPSCoR Cooperative Agreement #OIA-1655221.

402 *Data availability statement.* All the data and the codes used to plot results can be downloaded
403 via Brown University's digital archive DOI: [urlplaceholder](#).

404 **References**

405 Beardsley, R. C., and C. Chen, 2014: Northeast coastal ocean forecast system (necofs): A multi-
406 scale global-regional-estuarine fvcom model. *AGUFM*, **2014**, OS23C–1211.

- 407 Brissaud, J. B., 2005: The meanings of entropy. *Entropy*, **7 (1)**, 68–96, doi:10.3390/e7010068.
- 408 Carcassi, G., C. A. Aidala, and J. Barbour, 2019: Variability as a better characterization of shannon
409 entropy. *arXiv preprint arXiv:1912.02012*.
- 410 Correa, C. D., and P. Lindstrom, 2013: The mutual information diagram for uncertainty visualiza-
411 tion. *International Journal for Uncertainty Quantification*, **3 (3)**.
- 412 Cover, T. M., 1999: *Elements of information theory*. John Wiley & Sons.
- 413 DelSole, T., and M. K. Tippett, 2007: Predictability: Recent insights from information theory.
414 *Reviews of Geophysics*, **45 (4)**.
- 415 Deser, C., and Coauthors, 2020: Insights from earth system model initial-condition large ensembles
416 and future prospects. *Nature Climate Change*, 1–10.
- 417 Frankcombe, L. M., M. H. England, M. E. Mann, and B. A. Steinman, 2015: Separating internal
418 variability from the externally forced climate response. *Journal of Climate*, **28 (20)**, 8184–8202.
- 419 Franzke, C. L., and Coauthors, 2020: The structure of climate variability across scales. *Reviews of*
420 *Geophysics*, **58 (2)**, e2019RG000 657.
- 421 Hartley, R. V. L., 1928: Transmission Information. *Bell System Technical Journal*, **7 (3)**, 535–563.
- 422 Hawkins, E., and R. Sutton, 2012: Time of emergence of climate signals. *Geophysical Research*
423 *Letters*, **39 (1)**.
- 424 Jaynes, E. T., 1962: Information theory and statistical mechanics. Brandies University Summer
425 Institute Lectures in Theoretical Physics.
- 426 Kleeman, R., 2002: Measuring dynamical prediction utility using relative entropy. *Journal of the*
427 *atmospheric sciences*, **59 (13)**, 2057–2072.

428 Kowal, R. R., 1971: 296. note: Disadvantages of the generalized variance as a measure of
429 variability. *Biometrics*, **27 (1)**, 213–216, URL <http://www.jstor.org/stable/2528939>.

430 Leroux, S., T. Penduff, L. Bessières, J.-M. Molines, J.-M. Brankart, G. Sérazin, B. Barnier, and
431 L. Terray, 2018: Intrinsic and atmospherically forced variability of the amoc: insights from a
432 large-ensemble ocean hindcast. *Journal of Climate*, **31 (3)**, 1183–1203.

433 Leung, L.-Y., and G. R. North, 1990: Information theory and climate prediction. *Journal of*
434 *Climate*, **3 (1)**, 5–14.

435 Liang, Y.-c., and Coauthors, 2020: Quantification of the arctic sea ice-driven atmospheric circula-
436 tion variability in coordinated large ensemble simulations. *Geophysical Research Letters*, **47 (1)**,
437 e2019GL085397.

438 Llovel, W., T. Penduff, B. Meyssignac, J.-m. Molines, L. Terray, L. Bessières, and B. Barnier,
439 2018: Contributions of atmospheric forcing and chaotic ocean variability to regional sea level
440 trends over 1993–2015. *Geophysical Research Letters*, **45 (24)**, 13–405.

441 Majda, A. J., and B. Gershgorin, 2010: Quantifying uncertainty in climate change science through
442 empirical information theory. *Proceedings of the National Academy of Sciences*, **107 (34)**,
443 14958–14963.

444 Milinski, S., N. Maher, and D. Olonscheck, 2019: How large does a large ensemble need to be.
445 *Earth Syst. Dynam. Discuss.*, 2019, 1–19, doi: 10.5194/esd-2019, **70**.

446 Sane, A., B. Fox-Kemper, D. Ullman, C. Kincaid, and L. Rothstein, 2020: Consistent predictability
447 of the ocean state ocean model (osom) using information theory and flushing timescales. *Earth*
448 *and Space Science Open Archive*, 34, doi:10.1002/essoar.10504826.1, URL [https://doi.org/10.](https://doi.org/10.1002/essoar.10504826.1)
449 [1002/essoar.10504826.1](https://doi.org/10.1002/essoar.10504826.1).

- 450 Schneider, T., and S. M. Griffies, 1999: A conceptual framework for predictability studies. *Journal*
451 *of climate*, **12 (10)**, 3133–3155.
- 452 Schurer, A. P., G. C. Hegerl, M. E. Mann, S. F. Tett, and S. J. Phipps, 2013: Separating forced from
453 chaotic climate variability over the past millennium. *Journal of Climate*, **26 (18)**, 6954–6973.
- 454 Shannon, C., 1948: A Mathematical Theory of Communication. *Bell System Technical Journal*,
455 **27 (April 1928)**, 379–423,623–656, URL [http://math.harvard.edu/~ctm/home/text/others/](http://math.harvard.edu/~ctm/home/text/others/shannon/entropy/entropy.pdf)
456 [shannon/entropy/entropy.pdf](http://math.harvard.edu/~ctm/home/text/others/shannon/entropy/entropy.pdf).
- 457 Shchepetkin, A. F., and J. C. McWilliams, 2005: The regional oceanic modeling system (roms): a
458 split-explicit, free-surface, topography-following-coordinate oceanic model. *Ocean modelling*,
459 **9 (4)**, 347–404.
- 460 Stevenson, S., B. Rajagopalan, and B. Fox-Kemper, 2013: Generalized linear modeling of the el
461 niño/southern oscillation with application to seasonal forecasting and climate change projections.
462 *Journal of Geophysical Research: Oceans*, URL <http://dx.doi.org/10.1002/jgrc.20260>, in press.
- 463 Stone, J. V., 2015: *Information theory: a tutorial introduction*. Sebtel Press.
- 464 Waldman, R., S. Somot, M. Herrmann, F. Sevault, and P. E. Isachsen, 2018: On the chaotic
465 variability of deep convection in the mediterranean sea. *Geophysical Research Letters*, **45 (5)**,
466 2433–2443.
- 467 Yettella, V., J. B. Weiss, J. E. Kay, and A. G. Pendergrass, 2018: An ensemble covariance framework
468 for quantifying forced climate variability and its time of emergence. *Journal of Climate*, **31 (10)**,
469 4117–4133.

470 **LIST OF TABLES**

471 **Table 1.** Different types of forcing combinations employed to test their effect on vari-
472 ability. FF stands for full forcing: winds, tides, rivers, etc. For more details see
473 Sane et al. (2020). MR: mean rives; ZR: zero rivers; ZW: zero wind. 24

| Forcing Set | Wind forcing | River forcing |
|-------------|--------------|------------------|
| FF | NAM | As Observed |
| NECOFS | NECOFS | As Observed |
| MR | NAM | Time-averaged |
| ZR | NAM | Zero river input |
| ZW | Zero winds | As Observed |

474 TABLE 1. Different types of forcing combinations employed to test their effect on variability. FF stands for full
475 forcing: winds, tides, rivers, etc. For more details see Sane et al. (2020). MR: mean rives; ZR: zero rivers; ZW:
476 zero wind.

477 **LIST OF FIGURES**

478 **Fig. 1.** A sketch of a typical ocean or climate model output for an arbitrary variable. Each ensemble
479 is shown in different color and the mean of the ensemble is shown as black line. The model
480 mean can be considered to be the trend set by external forcings. The model spread shown by
481 double headed magenta arrow indicates the model chaos. 26

482 **Fig. 2.** Information theory metric of intrinsic vs. extrinsic variability γ as a function of correlation
483 coefficient in idealized Gaussian correlated arrays. The horizontal axis is the correlation
484 coefficient between mean member and ensemble members. The vertical axis shows the
485 information theory metric γ from (3) and the traditional metric γ_{std} from (4). A second
486 related experiment adding (50 out of 10,000) “corrupted” outliers to each individual member
487 is also shown. The information theory metric γ does not change for these outliers which
488 shows its robustness while γ_{std} is highly sensitive. 27

489 **Fig. 3.** Grid point wise kurtosis for OSOM output. Kurtosis is not closer to zero within (-0.5, 0.5)
490 suggesting the data distribution is non Gaussian. 28

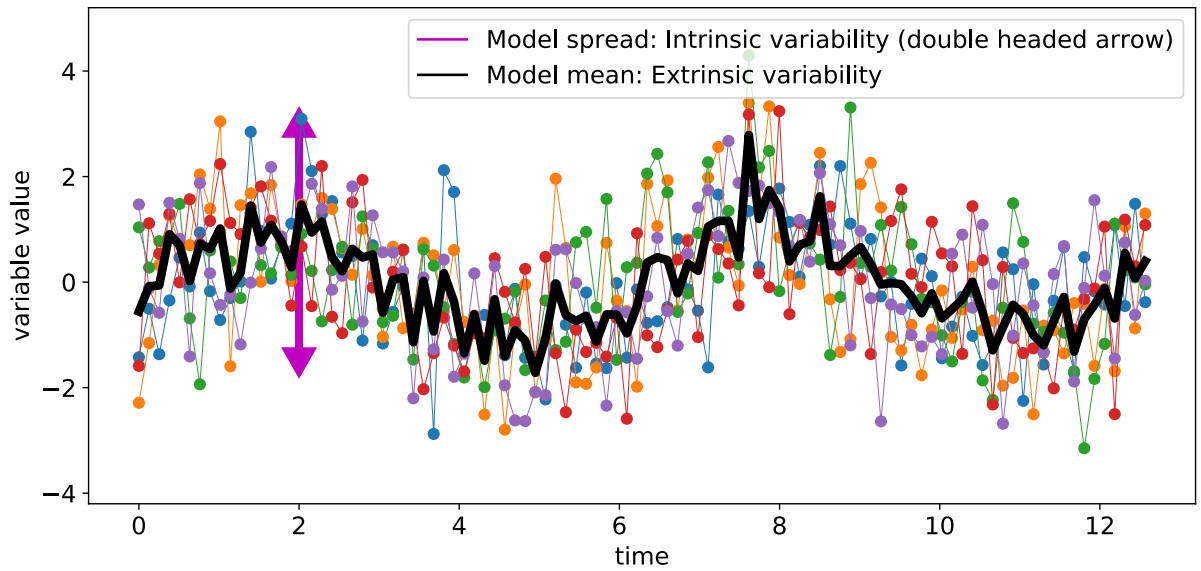
491 **Fig. 4.** Metrics γ vs γ_{std} for OSOM output. Both metrics show different contribution of intrinsic
492 variability to total variability. γ is more uniform throughout the domain than γ_{std} . Colormaps
493 for γ and γ_{std} are different to highlight the different ranges each of them have. γ_{std} for bottom
494 temperature has maximum value of 5%, and pattern is almost uniform except at the river
495 sources where values are on the lower side (less than 1%). 29

496 **Fig. 5.** Top: Intrinsic to total variability percentage for sea surface temperature. Bottom: Excess
497 kurtosis and skewness of the model mean of temperature at each grid point. Values closer
498 to zero (within 0.5 of zero, purple shades) are considered approximately Gaussian. The
499 deviation of model mean away from non normality implies that the ensemble members are
500 also non normal. The Arctic regions have the most skewness and excess kurtosis implying
501 non-Gaussian distributions. 30

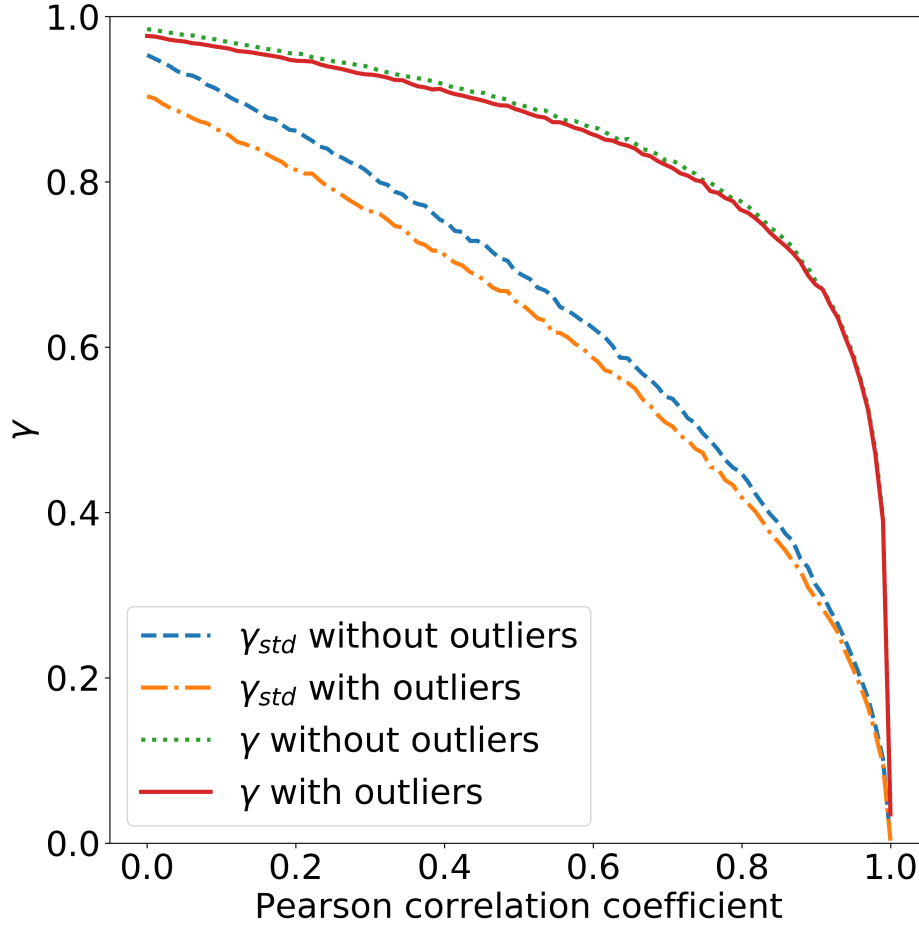
502 **Fig. 6.** Top: Intrinsic to total variability percentage for sea surface salinity. Bottom: Kurtosis and
503 skewness of the model mean of salinity at each grid point. Values closer to zero (within 0.5
504 of zero, purple shades) are considered approximately Gaussian. 31

505 **Fig. 7.** Shannon entropy applied to temperature and salinity. Replacing fully time varying rivers with
506 monthly-mean river flow gives almost the same result for salinity. Same is true by replacing
507 wind product with a different one. Rivers set to zero affects salinity but not temperature.
508 Winds are important in terms of variability but different wind products do not noticeably
509 alter variability. 32

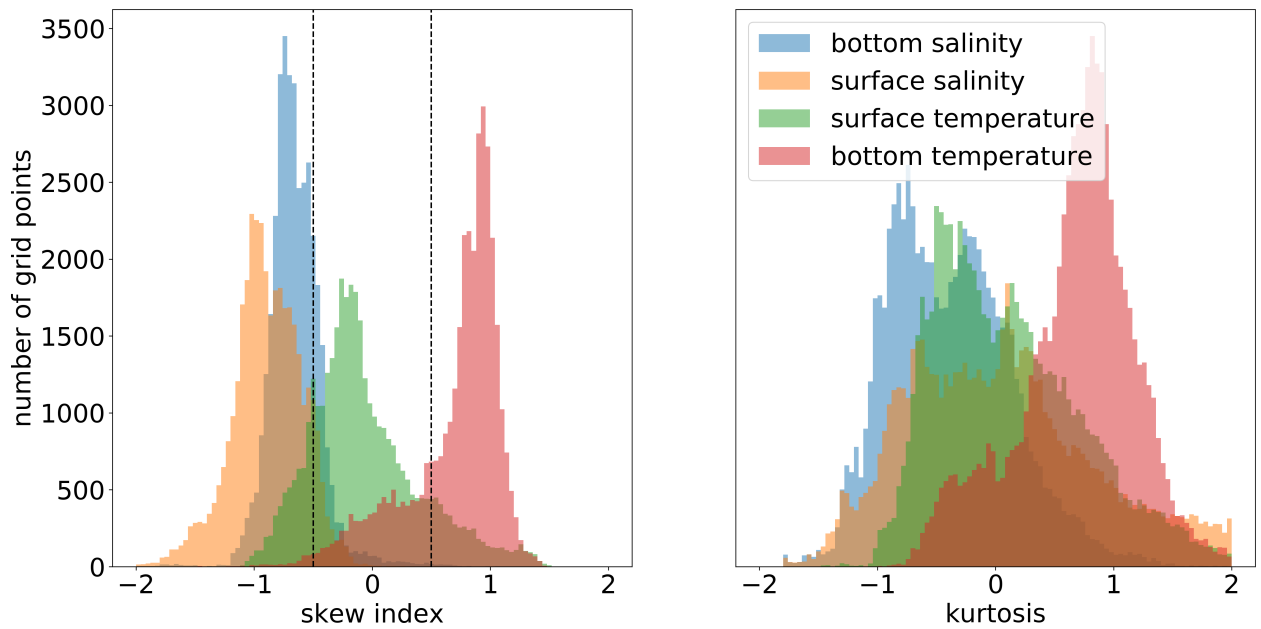
510 **Fig. 8.** Mutual information applied to simulations from different forcings. Higher mutual informa-
511 tion implies higher similarity in terms of variability. For example NAM-NECOFS values
512 are higher than NAM-ZW implying that NAM and NECOFS are significantly different than
513 having no wind. 33



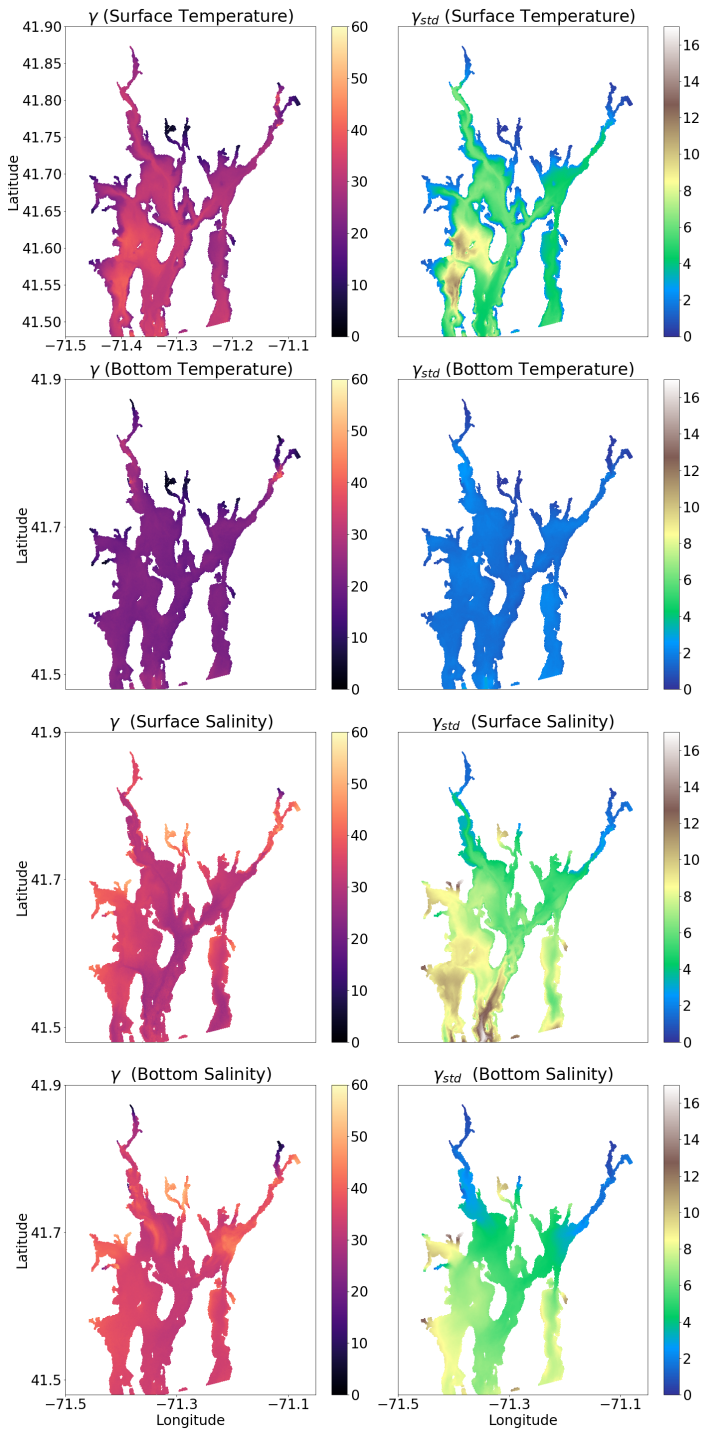
514 FIG. 1. A sketch of a typical ocean or climate model output for an arbitrary variable. Each ensemble is shown
 515 in different color and the mean of the ensemble is shown as black line. The model mean can be considered to
 516 be the trend set by external forcings. The model spread shown by double headed magenta arrow indicates the
 517 model chaos.



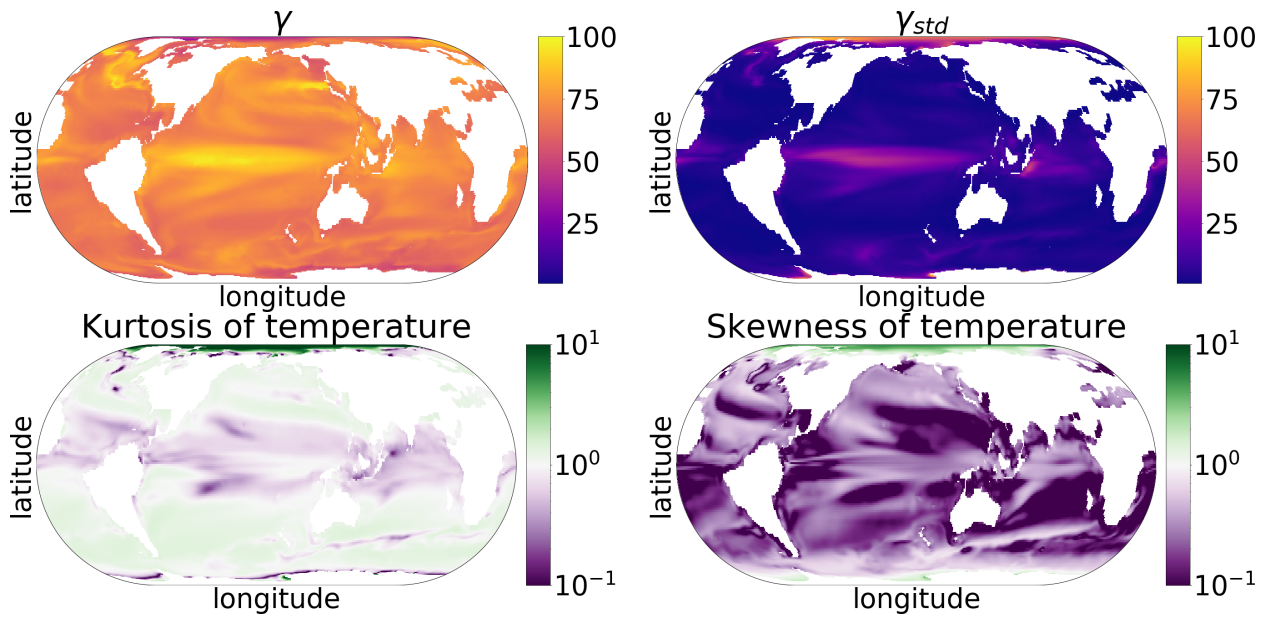
518 FIG. 2. Information theory metric of intrinsic vs. extrinsic variability γ as a function of correlation coefficient
 519 in idealized Gaussian correlated arrays. The horizontal axis is the correlation coefficient between mean member
 520 and ensemble members. The vertical axis shows the information theory metric γ from (3) and the traditional
 521 metric γ_{std} from (4). A second related experiment adding (50 out of 10,000) “corrupted” outliers to each
 522 individual member is also shown. The information theory metric γ does not change for these outliers which
 523 shows its robustness while γ_{std} is highly sensitive.



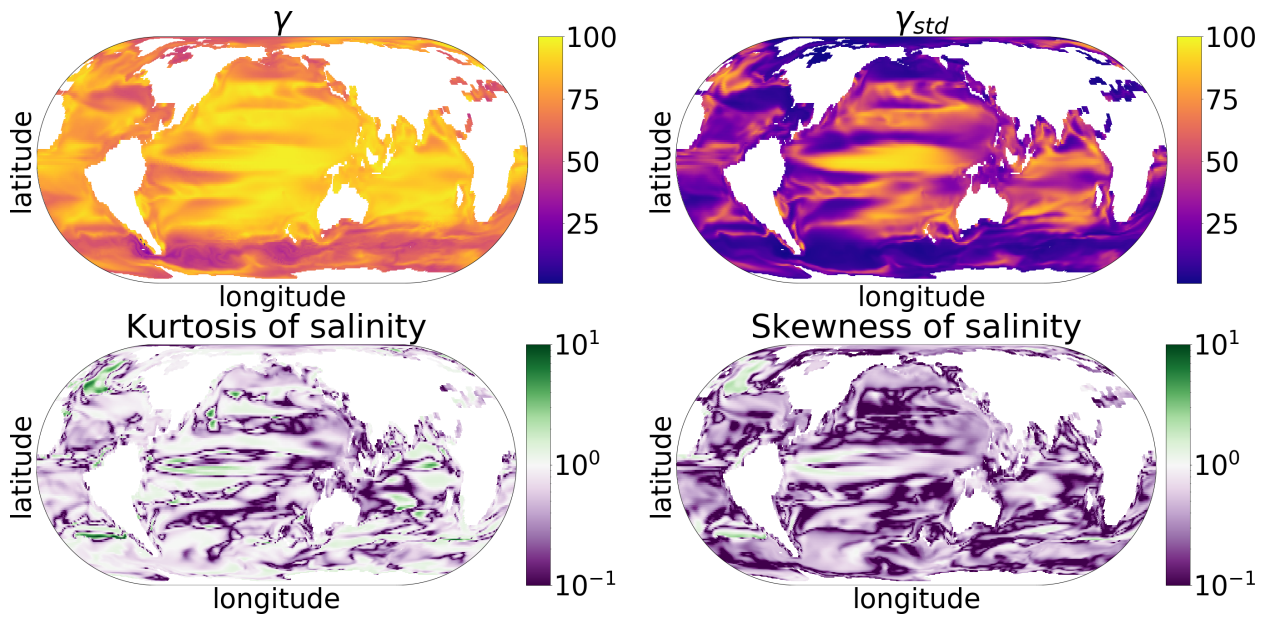
524 FIG. 3. Grid point wise kurtosis for OSOM output. Kurtosis is not closer to zero within $(-0.5, 0.5)$ suggesting
 525 the data distribution is non Gaussian.



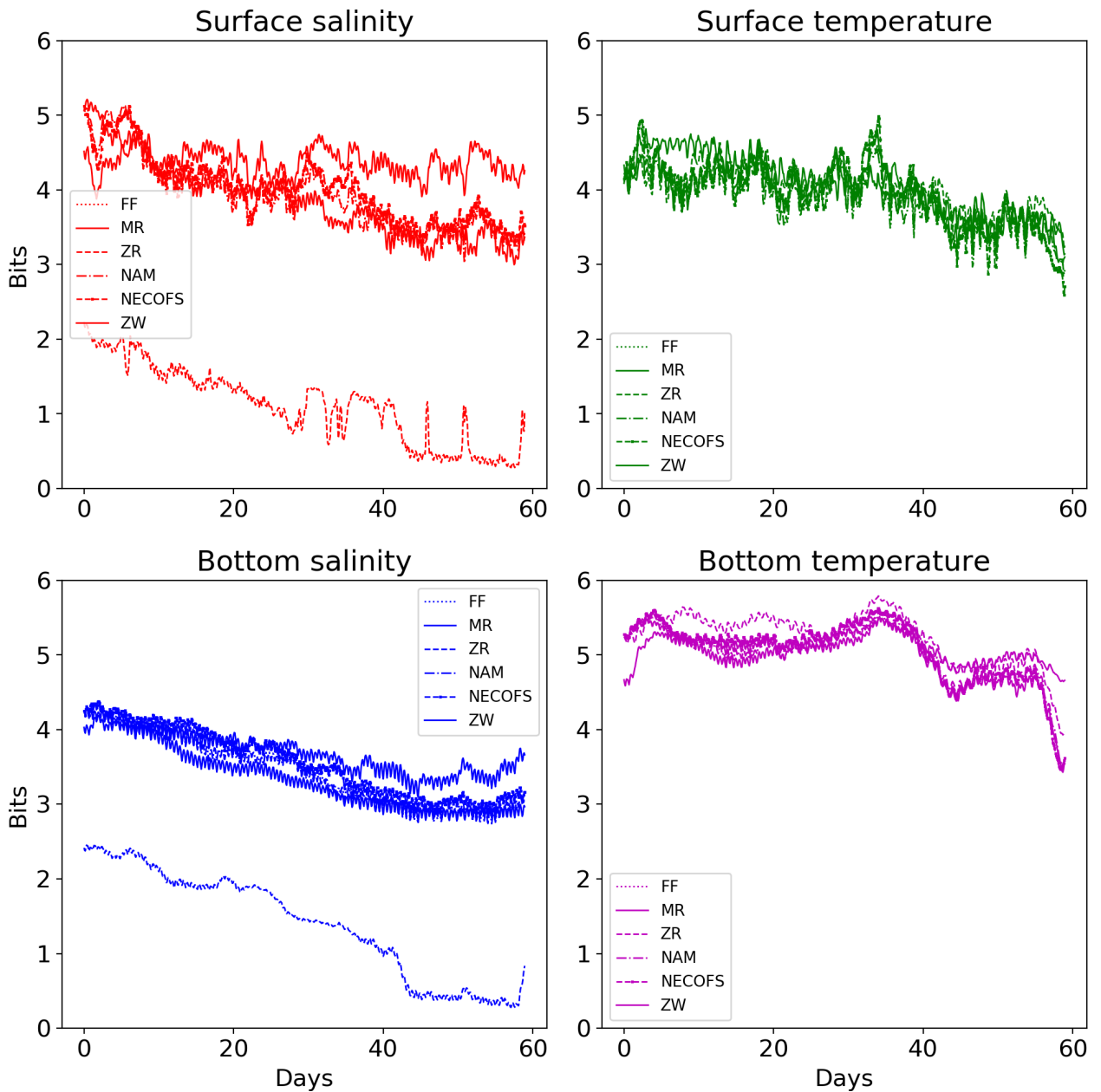
526 FIG. 4. Metrics γ vs γ_{std} for OSOM output. Both metrics show different contribution of intrinsic variability
 527 to total variability. γ is more uniform throughout the domain than γ_{std} . Colormaps for γ and γ_{std} are different
 528 to highlight the different ranges each of them have. γ_{std} for bottom temperature has maximum value of 5%, and
 529 pattern is almost uniform except at the river sources where values are on the lower side (less than 1%).



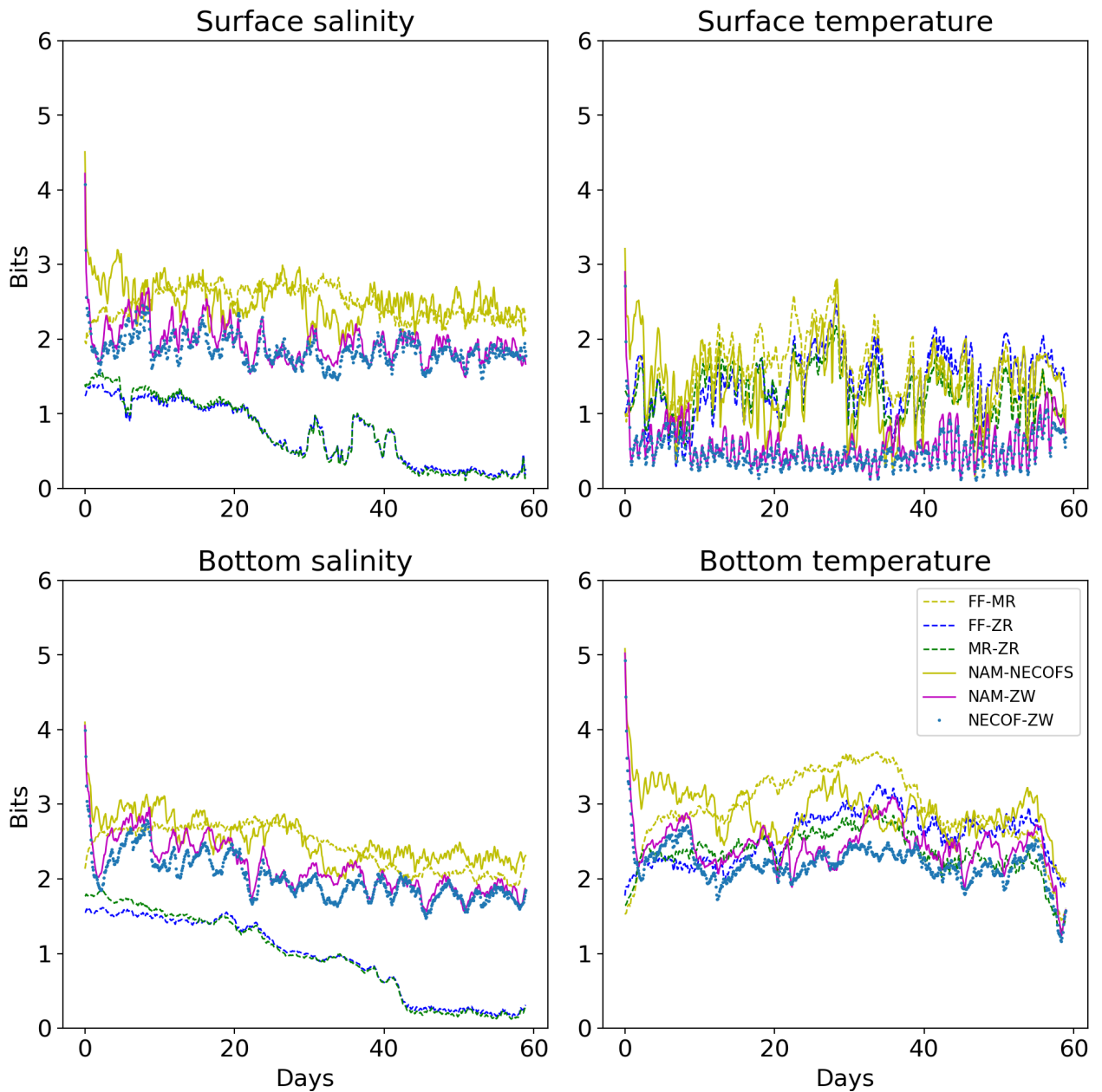
530 FIG. 5. Top: Intrinsic to total variability percentage for sea surface temperature. Bottom: Excess kurtosis and
 531 skewness of the model mean of temperature at each grid point. Values closer to zero (within 0.5 of zero, purple
 532 shades) are considered approximately Gaussian. The deviation of model mean away from non normality implies
 533 that the ensemble members are also non normal. The Arctic regions have the most skewness and excess kurtosis
 534 implying non-Gaussian distributions.



535 FIG. 6. Top: Intrinsic to total variability percentage for sea surface salinity. Bottom: Kurtosis and skewness
 536 of the model mean of salinity at each grid point. Values closer to zero (within 0.5 of zero, purple shades) are
 537 considered approximately Gaussian.



538 FIG. 7. Shannon entropy applied to temperature and salinity. Replacing fully time varying rivers with monthly-
 539 mean river flow gives almost the same result for salinity. Same is true by replacing wind product with a different
 540 one. Rivers set to zero affects salinity but not temperature. Winds are important in terms of variability but
 541 different wind products do not noticeably alter variability.



542 FIG. 8. Mutual information applied to simulations from different forcings. Higher mutual information implies
 543 higher similarity in terms of variability. For example NAM-NECOFS values are higher than NAM-ZW implying
 544 that NAM and NECOFS are significantly different than having no wind.